Available online at www.sciencedirect.com

SCIENCE DIRECT

Developmental Biology 279 (2005) 244–251

DEVELOPMENTAL BIOLOGY

www.elsevier.com/locate/ydbio

Cyclin D involvement demarcates a late transition in *C. elegans* embryogenesis

Judith Yanowitz[a,*], Andrew Fire[b]

[a]*Carnegie Institution of Washington, Department of Embryology, 115 West University Parkway, Baltimore, MD 21218, USA*
[b]*Departments of Pathology and Genetics, Stanford University School of Medicine, 300 Pasteur Drive-L235, Stanford, CA 94305, USA*

Received for publication 4 September 2004, revised 23 November 2004, accepted 16 December 2004
Available online 15 January 2005

Abstract

During development, progression through the cell cycle must be coordinately regulated with cellular differentiation. Despite significant progress in identifying genes required independently for each of these processes, the molecules which facilitate this cross talk have for the most part been elusive. Using the six macrophage-like coelomocytes of the nematode *Caenorhabditis elegans* as a model system to gain insight into the mesodermal differentiation pathway, we have isolated a set of mutants that alter coelomocyte numbers. One of these mutations, *cc600*, apparently results from a partial loss-of-function in the *C. elegans* cyclin D gene, *cyd-1*. The mutant has coelomocyte-specific defects without changes in other lineages. The mutants show that cell growth, terminal differentiation and cellular function proceed in the absence of *cyd-1* activity and cell division. The results suggest that certain mesodermal lineages may be uniquely affected by changes in *cyd-1* activity.

Keywords: Coelomocytes; Cell cycle; Cyclin D

Introduction

Nematode development provides an excellent model system for studying the relationships and connections between cell growth, cell division and cellular differentiation (Sulston and Horvitz, 1977; Sulston et al., 1983). In the initial phase of embryogenesis, a single zygote is cleaved into smaller and smaller progeny cells until cellular volumes ~0.2% of the original cell are obtained. Overt differentiation is absent during the early phases of this cleavage program; at later stages, cellular populations begin to take on the morphological and molecular characteristics reflective of their final fate. Larval development entails a much more limited set of cell divisions, with a few blast cells (many of which already exhibit differentiated characteristics) undergoing repeated rounds of cell growth and division (Sulston and Horvitz, 1977). Furthermore, in larval development, there is extensive growth of many of the post-mitotic cells in the animal, so that the volume of a differentiated body wall muscle cell in an adult can be several orders of magnitude greater than that of the same cell in a newly hatched larva. The picture that emerges from these observations is that of flexibility in the relationship between cell growth and cell division. Although *C. elegans* provides a robust example of such analysis, this overall picture is by no means unique to the nematode system. Indeed, amphibian development provides examples in which a very similar profile of cell growth and division can produce a vertebrate animal (Chan and Etkin, 2001).

The interface between the non-growth-linked early divisions in the nematode embryo and later (apparently growth-linked) divisions in larvae is of considerable interest. We have initiated a genetic approach to the analysis of growth and patterning for a small set of cells that exemplify this developmental interface. Nematode coelomocytes are

* Corresponding author. Fax: +1 410 243 6311.
E-mail address: jly@alum.mit.edu (J. Yanowitz).

0012-1606/$ - see front matter © 2004 Elsevier Inc. All rights reserved.
doi:10.1016/j.ydbio.2004.12.022

non-muscle mesodermal cells found in the pseudocoelomic space between the intestine and the body wall. These cells have been proposed to play a scavenger role, based on their ability to continuously endocytose low molecular weight dyes and proteins (e.g. GFP) and to extracellularly accumulate larger materials from the body cavity (Chitwood and Chitwood, 1950; Fares and Greenwald, 2001a). These observations suggest that coelomocytes may serve certain immune or hepatic functions for *C. elegans*. However, unlike immune cells in other organisms, the coelomocytes are not migratory; rather, they are attached to the hypodermis, and would rely on the movement of the animal to bring foreign agents into their proximity.

The six coelomocytes in the hermaphrodite are derived from two parts of the mesodermal lineage (see Fig. 1A): four are born during embryogenesis from MS lineage (Sulston et al., 1983); two are post-embryonically derived from divisions of the M blast cell (Sulston and Horvitz, 1977). In hermaphrodites, the four embryonic coelomocytes lie on the ventral side between the pharynx and vulva, and the two post-embryonic, M-derived coelomocytes reside dorsally in the tail (Fig. 1A). In males, one of the germ line proximal coelomocytes migrates to reside more posteriorly, and only one M-derived coelomocyte is formed. The four embryonic coelomocytes arise from two precursor cells that divide equally, late in embryogenesis. At this stage in development, most of the embryonic cell divisions have been completed. The coelomocyte lineages present several fundamental questions about developmental programs, including how two different lineages can give rise to the same terminal phenotype, whether division of the embryonic mother cell is required for its differentiation, whether the prolonged growth arrest of this cell is necessary for terminal differentiation, and if and how cell migration is coordinated to terminal differentiation.

The parts of the mesodermal lineage from which the coelomocytes arise respond to both cell intrinsic and extrinsic contributions to fate decisions. Although many of the genes required for muscle cell fates have been well characterized, the genes required for the distinction between muscle and non-muscle cell fates have not been identified. Several characteristics of coelomocytes make these cells

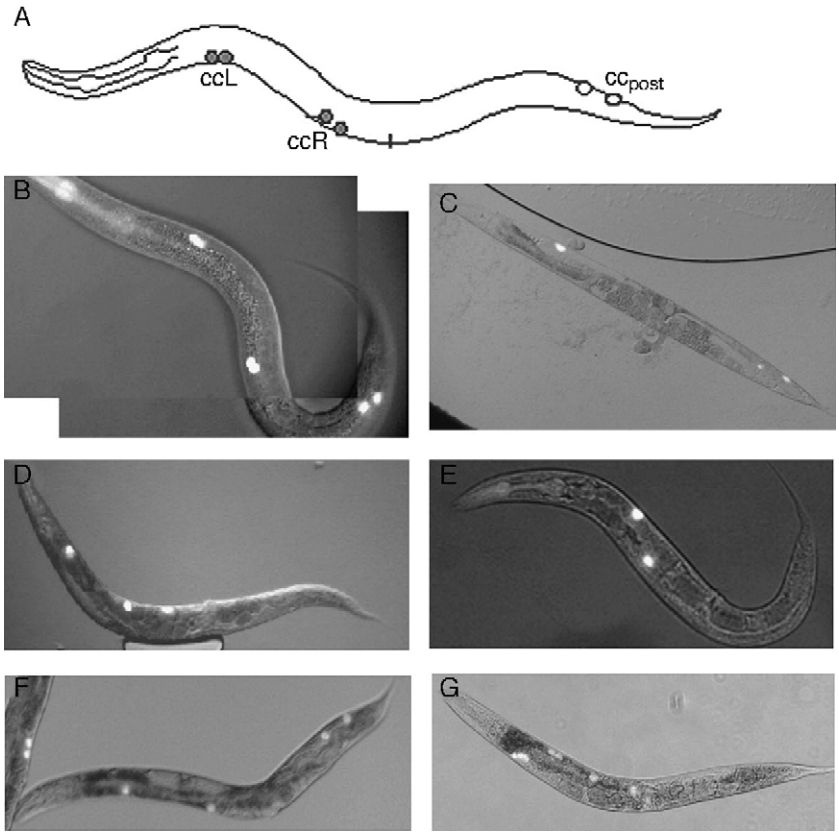

Fig. 1. Mutants defective for specification of the embryonic coelomocytes. Wild type animals (A, B) have six coelomocytes: the pair near the head are on the left side of the animal (ccL) and the pair near the vulva, in middle of the animal, on the right side (ccR) are born during embryogenesis; the two in the tail (cc_{post}) are born during larval cell divisions. (C) *cc591* shows a lineage-specific defect, missing the pair of coelomocytes near the vulva. (D) *cc589* and (E) *unc-39* show variable numbers of coelomocytes with loss from either or both the embryonic and post-embryonic lineages. (F) *cc600* displays a defect in division of the embryonic mother cells, such that the adults have four total coelomocytes, two of embryonic origin and two post-embryonic. (G) *cc588* and *cc593* (not shown) display an increased number of coelomocytes with a maximum of twelve total. These mutations also have a coelomocyte migration defect with the majority of coelomocytes residing more anteriorly. (B, D, E) Coelomocytes are marked with the *twist::GFP* intrinsic reporter which also gives background fluorescence in the pharynx. (C, F, G) Coelomocytes are marker with *myo-3::sGFP* which is a functional reporter and relies on the uptake by the coelomocytes of GFP secreted into the coelomic cavity by muscle cells.

particularly amenable to genetic study. First, both molecular and functional markers for the coelomocyte cell are available. Second, the organism tolerates deviations in the number of coelomocytes (Greenwald and Seydoux, 1990; Harfe et al., 1998). Third, the small number of coelomocytes (six) facilitates screening mutants for changes in numbers.

We report here the initial identification and characterization of a set of mutations that affect coelomocyte number, specification and morphology. Further molecular analysis of one of these mutations has revealed a role for cyclin D in the late embryonic cell divisions that are unique to the coelomocyte lineage. Our characterization of this mutation indicates that terminal differentiation into the embryonic coelomocytes can occur without the final cell divisions and that cell growth proceeds without cyclin D or DNA replication. In addition, the observation that only coelomocytes fates are altered in this mutant suggests the possibility of differential requirements for *cyd-1* in different cell lineages.

Materials and methods

C. elegans methods

Standard genetic protocols for *C. elegans* (Brenner, 1973) were used, with all analyses performed at 20°C. The following mutations were used in the genetic analyses: *dpy-5(e61)*I, *unc-13(e1091)*I, *dpy-10(e128)*II, *rol-1(e91)*II, *unc-52(e444)*II, *dpy-18(e364)*III *unc-32(e189)*III, *unc-17(e245)*IV, *dpy-4(e1166)*IV, *dpy-11(e224)*V, and *unc-46(e177)*V (Brenner, 1973); *cyd-1(he112)*II (Boxem and van den Heuvel, 2001), *mom-3(or78)*II (Thorpe et al., 1997), *lin-7(e1413)*II (Herman et al., 1980), and *him-5(e1490)*V (Hodgkin et al., 1979). *mnC1[dpy-10(e128)unc-52(e444)]*II is a balancer chromosome for the right side of chromosome II.

The following integrated transgenes were used as additional genetic markers and to evaluate mesodermal tissues in wild type and mutant animals. Expression patterns are as noted: *ccIs4251*[*myo-3*::*gfp*]*I* (Kostas and Fire, 2002): all body wall muscles; *ayIs6*[*hlh-8*::*gfp*]*X* (Harfe et al., 1998): lineal derivatives of the post-embryonic myoblast M; *ccIs4443*[*arg-1*::*gfp*]*IV* (Kostas and Fire, 2002): head mesodermal cell and vulval muscles; *ayIs2*[*egl-15*::*gfp*]*IV* (Kostas and Fire, 2002): vm1 vulval muscles; *arIs37*[*pmyo-3*::*ssGFP*]I: GFP secreted from muscle cells expressing this construct accumulates in coelomocytes. A second mutation (*cup-5(ar465)*III (Fares and Greenwald, 2001b) was used to increase the GFP signal in *arIs37*-carrying strains; *ccIs4438* [*hlh-8*::*gfp*]*IV*: an enhancer from the *twist* gene drives coelomocyte-specific *gfp* expression (Harfe et al., 1998).

Cloning and sequence analysis of cc600

Mutants with altered coelomocyte patterns were isolated in F_2 and F_3 progeny following mutagenesis of *arIs37[pmyo-3*::*ssGFP]I; cup-5(ar465)III*. Mutant lesions responsible for the observed coelomocyte pattern defects were then mapped to linkage groups with visible Dpy Unc markers (see Table 1). Based on the map position of mutant cc600, the cyclin D gene *cyd-1* (promoter region, coding region and 3′UTR) was amplified in 1 to 1.5 kb overlapping PCR fragments and sequenced on both strands.

We characterized the molecular consequences of *cc600* by performing RT–PCR analysis on mRNAs from wild type, *cc600*, and the parental strain *arIs37[pmyo-3*::*ssGFP]*I; *cup-5(ar465)*III. One plate each of starved animals were washed off 6 cm plates with M9 buffer (Brenner, 1974), sedimented, frozen at −70°C, thawed and extracted with Trizol (Invitrogen) as directed. mRNAs were suspended in 10 mM Tris (pH 7.5) and 1 μl was used in subsequent reactions. RT reactions used primer AF-JLY445

Table 1
Mutations affecting embryonic coelomocyte specification

Allele	Coelomocyte phenotype	Penetrance	Linkage group	Other phenotypes
cc593	Increase (up to 12), occasional loss of post-embryonic ccs	~30%	IV	
cc588	Increase (up to 12), occasional loss of post-embryonic ccs	25–30%	?	Some sterility
cc589	Variable decrease (1–6 ccs)	80%	V	Uncoordinated, withered tail (wit)
unc-39	Variable decrease (1–6 ccs)	50–90%	V	unc, wit
cc590	Variable decrease (1–4 ccs)	25%	III	Endocytosis defect
cc600	Embryonic mother cells not divide (1 ccL, 1 ccR)	>90%	II	
cc591	Loss of ccR pair	25%	V	cc and DTC migration defects
cc595	Premature degradation, manifest in L3	>80%	N.D.	
cc596	Premature degradation, starts in L4		N.D.	
cc597	Premature degradation, manifests in adult	20%	N.D.	
cc598	Premature degradation, manifests in adult	>50%	N.D.	
cc599	Premature degradation, manifests in L3/L4	20–30%	N.D.	
cc601	Premature degradation, manifests in L3		N.D.	
cc602	Premature degradation, manifests in adult	<20%	N.D.	

Post-embryonic specification mutants are not listed.

GTACGAGTCGAGAAGGTTCACTTCC that spans an exon/exon boundary (so that genomic DNA would not be amplified) using AMV Reverse transcriptase (Promega) and standard conditions. PCR reactions used primers AF-JLY 443 TCGGAAACATCTATTACCGAG and AF-JLY-444 TTCGATACGTAGTAGAGGCCA, and were amplified for 35 cycles 95° 10 s, 55° 10 s, 72° 10 s in 20 μl reactions with ThermalAce polymerase (Invitrogen).

Assay for DNA content and cell size

Fluorescence of the DNA-binding dye DAPI in fixed animals was used to measure DNA content of individual nuclei. Microscopic images were acquired on a CCD camera taking care to keep intensities within the usable range of the detector. Raw measurements of DNA content (area of nucleus *x* mean intensity above background) were converted to "C-value" DNA content by internal comparison with measurements from muscle and neuronal nuclei (known DNA content 2C) and meiotic pachytene nuclei (DNA content of 4C) (Hedgecock and White, 1985). Cell volumes were measured from differential interference contrast (Nomarski) images of embryonic and post-embryonic coelomocytes. Long and short axis measurements of cell size were averaged and volumes calculated assuming ellipsoidal cell shape. Volume calculations were normalized relative to the embryonic coelomocytes in N2 animals.

Results

To identify genes that altered coelomocyte specification, we took advantage of a functional GFP reporter which effectively labels all coelomocytes based on their ability to endocytose GFP from the pseudocoelomic cavity. We also used a mutation, *cup-5(ar465)*, which is defective in metabolism of the endocytosed material and therefore excessive GFP accumulates in the vacuoles of the coelomocytes (Fares and Greenwald, 2001b). The coelomocytes are therefore easily visualized under a fluorescence stereomicroscope.

Following mutagenesis of *arIs37[pmyo-3::ssGFP]; cup-5(ar465)* animals with EMS, we screened F_1 and F_2 generations for animals with altered numbers of coelomocytes. In one screen, approximately 7300 F1 hermaphrodites (14,600 haploid genomes) and their clonal progeny were visually inspected for changes in coelomocyte number. An additional 47,000 F2 animals were examined in a non-clonal screen. Twenty-two independent coelomocyte specification mutants were obtained. All of the mutations appear to be recessive. Seven mutations affect the embryonic coelomocytes and each represents a separate complementation group, indicating that the screen was not performed to saturation and suggesting that a significant number of additional genes are likely to affect coelomocyte patterning.

Given that we identified only seven mutations in greater than 61,000 genomes screened, and the fact that none of the mutations are in the same complementation group, we infer that most of the genes required in the embryonic coelomocyte developmental program are not unique to this lineage. This further implies that the mutations that we have isolated are likely to be non-null alleles in genes with additional roles in other lineages.

To ensure that changes in coelomocyte number were not due to an altered ability of the coelomocytes or other cells to take up the secreted GFP, we replaced the muscle-expressed secreted gfp reporter (*myo-3::ssGFP*) with an intrinsic reporter (*ccIs4438* [see Materials and methods]) so that GFP is expressed within coelomocyte cells. Coelomocyte patterns in mutants were also assessed by scoring for the characteristic coelomocyte cell morphology directly using DIC (Nomarski) optics. For the mutants that we analyzed, identical numbers and patterns of coelomocytes were observed with the three methods.

The mutants fell into several phenotypic classes (see Table 1 and Figs. 1B–G): increased number of coelomocytes; random decrease in the number; lineage-specific decrease; and premature degradation. The lineage-specific decreases could further be classified by which coelomocytes were affected. These fell into three unique groups: defective in both pairs of embryonic coelomocytes; defective in the MSap-derived coelomocytes; defective in the post-embryonically derived coelomocytes. The isolation of different phenotypic classes underscores the power of such a screen in identifying mutations that affect multiple aspects of developmental control.

We were especially intrigued by the coelomocyte defect in *cc600* mutants. From visual inspection of these animals, it appeared as if the embryonic coelomocyte mother cells had not divided, but rather had directly differentiated into functional coelomocytes. This suggested that *cc600* might uncover a locus involved in coordinating cell cycle progression to terminal differentiation. In addition, inspection of these animals both by DIC microscopy and with the use of a panel of mesodermal GFP transgene reporters (data not shown) could identify no other morphological defects in these animals or their coelomocytes. The remainder of this report deals with the cloning and characterization of this mutation.

Molecular cloning of cc600, mutations and RNAi

The *cc600* mutation is highly penetrant, facilitating the mapping and characterization of the mutant phenotypes. We mapped *cc600* between *rol-1* and *lin-7* on LG II. Interpolation of the genetic data onto the physical map, placed the *cc600* lesion in the area of the single *C. elegans* gene encoding cyclin D. We sequenced the *cyclin D* gene from homozygous *cc600* mutant animals and identified a single nucleotide change in the conserved splice donor site in intron 2 (Fig. 2A). No additional lesions were identified

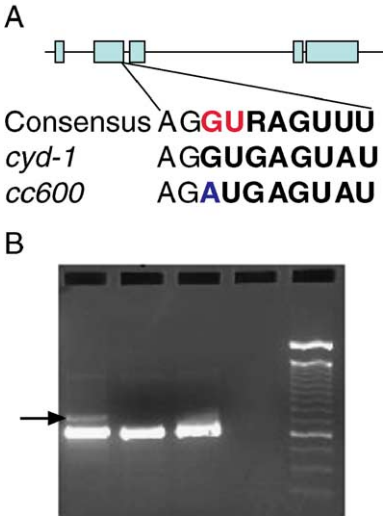

Fig. 2. *cc600* is a mutation in the *cyd-1* gene. (A) Schematic of the *cyd-1* genomic region. The *cc600* lesion is a G to A transition at the conserved GU at the beginning of the first intron. The *C. elegans* consensus sequence for the exon/intron boundary is shown (Blumenthal and Steward, 1997), as is the sequence in the wild type *cyd-1* gene and the *cc600* mutant. (B) RT–PCR analysis indicated the prevalence of a weak additional band in the *cc600* mutant (arrow), but not in the *cup-5; myo-3::sGFP* parent nor in wild type N2 animals. The increase in size of the band corresponds precisely to the size of intron 2 and sequencing confirmed its identity.

in the coding region, the 5 kb upstream of the start site or 500 bp downstream of the stop codon.

RT–PCR analysis of poly A+ RNA from *cc600* animals confirmed the presence of spliced and unspliced RNA species in these animals whereas only spliced product could be detected in wild type animals (Fig. 2B). Sequencing of these RT–PCR products confirmed that the unspliced RNAs from the mutant animals contained the transition expected from the mutant DNA sequence. These results suggest that *cc600* is a bona fide splice site mutation in the second intron of cyclin D.

Although this mutation changes the splice site sequence from the consensus, this novel splice site is not expected to completely abrogate splicing at this position. Rather it is likely to reduce the efficiency with which this site is utilized (Roca et al., 2003). This may have two consequences at the molecular level. First, it may allow for usage of an alternative splice donor site 4 base pairs upstream to be utilized. This would produce a frameshift and likely this mutation would be subject to nonsense-mediated decay through the *smg* pathway. Although this is a possible outcome, our RT–PCR and sequence analysis did not show any transcripts which utilized this cryptic splice site. The second possible defect resulting from this base transition is a failure to utilize the splice site, thus allowing for the accumulation of unspliced transcripts (as detected by our RT–PCR analysis). The unspliced products would also produce premature stop codons and be subject to *smg*-mediated decay. Consistent with this possibility, as mentioned above, we detected unspliced mRNAs in the mutant animals. That this transcript may be *smg*-sensitive is reflected in the small percentage of unspliced relative to spliced transcripts that are detected. Given that we do not see a coelomocyte division defect in heterozygous null animals, we would have expected that at least 50% of transcripts produced in the *cc600* mutant should be aberrant; instead, only a small fraction of the transcripts detected are unspliced.

To further confirm that *cc600* is a mutation in the *cyclin D* gene, we made animals transheterozygous for *cc600* and *cyd-1(he116)*, a *cyclin D* null allele. *cyd-1(he116)* mutant animals are defective in all larval divisions (Park and Krause, 1999), as well as in the final few embryonic intestinal divisions (Boxem and van den Heuvel, 2001). Transheterozygotes *cyd(he116)/cc600* displayed the *cc600* coelomocyte phenotype (Fig. 3A) without any of the other cell cycle defects manifested in the

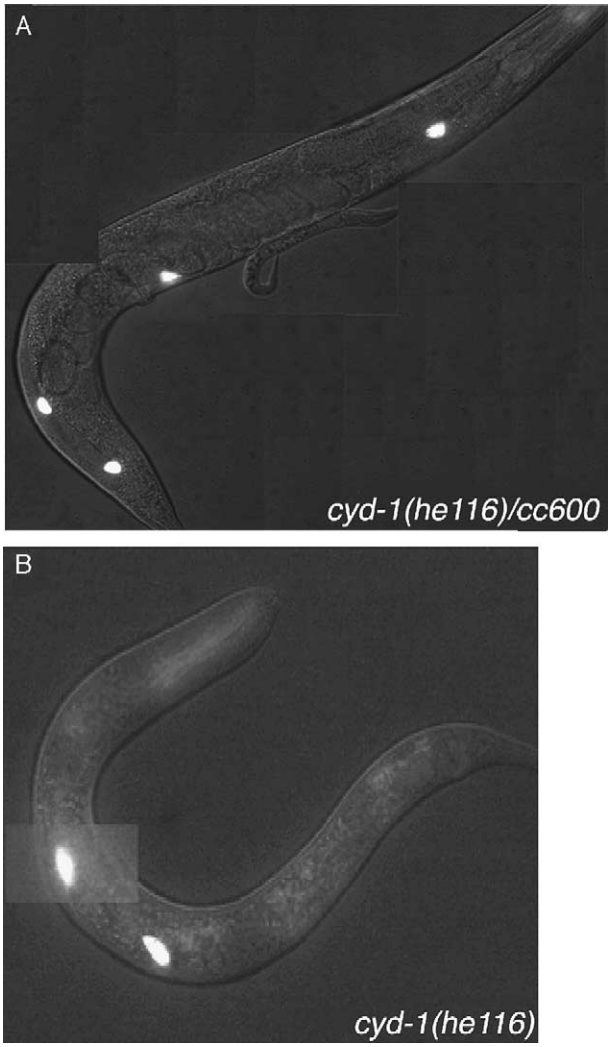

Fig. 3. *cc600* is allelic to *cyd-1*. Transheterozygous *cyd-1(he116)/cyd-1(cc600)* (A) and *cyd-1(he112)/cc600* (not shown) display the *cc600* coelomocyte defect; no additional cell cycle abnormalities were observed. (B) Homozygous *cyd-1(he116)*, *cyclin D* null animals, have two coelomocytes (shown as a merged image in the same focal plain), due to defects in the divisions of the embryonic coelomocyte mother cells, as well as all post-embryonic divisions.

null animals. This result underscores the cell type-specific defects of the *cc600* allele and suggests that coelomocytes might be particularly sensitive to reductions in cyclin D levels.

To further investigate the role of *cyclin D* in the coelomocytes and determine whether *cc600* defects were allele-specific, we examined the *cyd-1(he116)* homozygous mutant animals for coelomocyte defects. Since this mutation prevents all post-embryonic divisions, the mutant animals were expected to contain at most the four embryonic coelomocytes. As shown in Fig. 3B, *cyd-1(he116)* animals are missing the post-embryonic coelomocytes and only have two embryonic coelomocytes. As with the *cc600* mutant animals, these coelomocytes are larger than in wild type animals. Together with the positions of these coelomocytes near the pharynx and vulva, these data are consistent with a failure in coelomocyte mother cell divisions. Similar results were obtained using the loss of function allele *cyd-1(he112)*(Boxem and van den Heuvel, 2001) and *cyd-1(RNAi)* (data not shown).

cyd-1(cc600) separates cell cycle progression from cell growth

cyd-1 is required for G1/S progression and all *cyd-1* null animals arrest cell divisions prior to S phase. To further examine the cell cycle defect in the *cyd-1(cc600)* mutant animals, we DAPI stained *cyd-1(cc600)* mutant animals and quantitated the signal in the coelomocytes, and nearby muscle, neuronal, intestinal and germ cell nuclei. Whereas the nearby germ line meiotic nuclei gave the expected 4C signal in DAPI fluorescence, DAPI intensities in the undivided coelomocyte mother cells were 2C (no difference from control neuronal and muscle nuclei; Fig. 4A). These data are consistent with the coelomocyte mother cell arresting in G1.

Although the mother cell arrests in G1, the sizes of the cells are significantly larger than expected. In fact, the size of the mutant coelomocytes is almost exactly double that of either the post-embryonic coelomocytes in the same animals or the embryonic coelomocytes in wild type animals (see Fig. 4B). An alternative explanation for the increased size of the coelomocytes in *cc600* mutant animals is that in animals with decreased numbers of coelomocytes, each cell would be functionally more active and would accumulate more endocytic vesicles. To address this possibility, we examined *cc589* mutant animals that display a variable decrease in coelomocyte number. We assayed *cc589* mutant with four coelomocytes and did not observe a significant change in coelomocyte size in these mutants (Fig. 4B). Thus, we conclude that although the DNA cycle has arrested in G1 in *cyd-1(cc600)* mutant animals, the cell growth program has not been arrested. We observed no obvious cell growth defects in other tissues. However, the animals do appear slightly dumpy as compared to wild type. This observation suggests that other tissues might have a marginal response to the reduced *cyd-1* levels seen in *cc600* mutants.

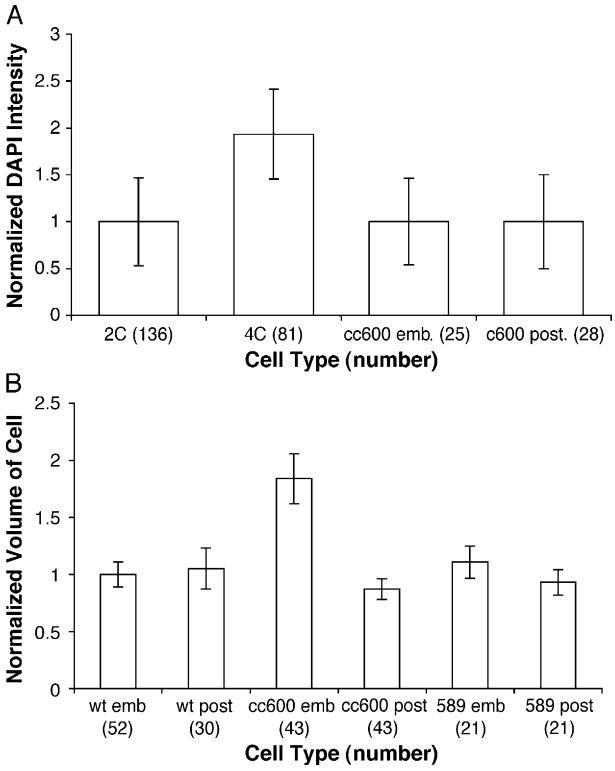

Fig. 4. *cyd-1(cc600)* mutants display defects in cell cycle progression but not cell growth. (A) Shown are the relative DAPI intensities of control 2C cells (muscle and neuronal nuclei), 4C cells (germline meiotic nuclei) and embryonically derived (cc600 emb) and post-embryonically derived (cc600 post) coelomocytes from *cyd-1(cc600)* mutant animals. For all measurements, $P < 0.005$. (B) Shown is the relative volume of the embryonically derived (emb) and post-embryonically derived (post) coelomocytes from *wild type* (wt), *cyd-1(cc600)* and *cc589* mutant young adults, $P < 0.005$. In both panels (A) and (B), the number in parentheses is the total number of cells measured.

Discussion

Coordination of cell cycle progression, cell fate specification and terminal differentiation are critical to the proper development of all multicellular eukaryotes. A screen for coelomocyte mutations identified a number of mutations that affect various steps in development of these cells. It is likely that further characterization of these mutations will shed significant insight into how this developmental program is initiated and elaborated. One interesting mutation that we isolated from this screen, *cc600*, gave a unique phenotype in that it affects the cell division of the embryonic coelomocytes with no obvious effects in the rest of the animal. The characterization of this mutation sheds light onto several aspects of coelomocyte fate specification in particular, and on cell cycle regulation in *C. elegans* in general.

It had previously been thought that cyclin D was dispensable for embryonic cell divisions in *C. elegans* because of the absence of a true G1 phase (Park and Krause, 1999). Our observations with *cyd-1(cc600)*, together with those of decreased intestinal cell divisions in the *cyd-1* null mutants (Boxem and van den Heuvel, 2001), suggest that late embryonic divisions have acquired a growth phase—presumably a true G1 phase. Nevertheless, our results do not rule out the possibility that growth is a consequence of the differentiation program, and that the growth we observe in the undivided coelomocyte mother cell is activated independently of cell division.

The coelomocytes are mesodermal cells that arise from two separate lineages (Fig. 1A). The embryonic coelomocytes are born in pairs from progeny of two different MS granddaughters, MSap and MSpp (Sulston et al., 1983). The post-embryonic coelomocytes arise from divisions of M blast cell and do not share a common parent (Sulston and Horvitz, 1977). Since each of the embryonic coelomocytes come from a precursor that divides evenly to give two coelomocytes, one question in regard to the cell fate decision is whether this cell division is actually required or whether the coelomocyte fate is determined earlier in development, at the asymmetric division that gives rise to the mother cell. This is of particular interest because the mother cell is born during the large burst of embryonic cell division and remains arrested for several hours before dividing into two coelomocytes. This makes the coelomocytes among the latest born embryonic cells in *C. elegans*, which suggested de facto that perhaps the developmental program was linked to this cell cycle arrest. In contrast, however, we found that the final cell divisions which produce two pairs of coelomocytes are not required to establish functional coelomocytes. Even in the absence of cell division, the mother cell switches on the terminal differentiation program.

It also appears that the coelomocyte mother cell may only have a small window of opportunity during which this final cell division can be initiated. In fact, our attempts to alter cyclin D (or cyclin E) levels by heat shock in newly hatched L1s were never able to rescue the coelomocyte-specific defect in cell cycle progression (data not shown). We interpret this to mean that once the cell has committed to terminal differentiation, it cannot reenter the cell cycle—at least not by the sole expression of a single G1 cyclin. These results with cyclin D in coelomocyte fate specification are similar to the results of Fay and Han (Fay and Han, 2000) for vulval precursor cell (VPC) differentiation and the role of cyclin E. Our results also suggest that perhaps an underlying timing mechanism may be initiated much earlier in development than had previously been documented. Perhaps the transition to a true G1 coincides with the onset of a developmental program linked to a heterochronic mechanism.

Mesodermal fate differentiation involves a precise pattern of gene expression that is coordinated with cell cycle exit. This is best understood for muscle differentiation where mitogen signaling coordinates the skeletal muscle differentiation program regulated by MyoD, myf-5 and Mef2d with cell cycle withdrawal. In mouse, cyclin D-cdk4 acts as a specific inhibitor both of MyoD to block interaction with DNA (Zhang et al., 1999) and also of Mef2C to inhibit its interaction with the coactivator Grip-1 (Lazaro et al., 2002). It is intriguing to speculate that the tissue-specific affects of the *cyclin D(cc600)* mutant will provide a link to similar regulatory controls in a different mesodermal tissue. Insight into the precise mechanism of coelomocyte arrest awaits the isolation and characterization of genetic suppressors of the *cc600* phenotype.

Boxem and van den Heuvel (2001) suggest that *cyd-1* primarily promotes cell cycle entry and does not have a significant role in regulating cell growth based on the timing of the growth versus cell cycle defects in intestinal cells. Our examination of the coelomocyte phenotype in cyclin D mutants leads to a similar interpretation. Although the *cyd-1(cc600)* results cannot rule out the interpretation that cell growth and cell cycle progression are sensitive to different levels of cyclin D protein, the absence of growth control in the cyclin D null background strongly supports an exclusive role in cell cycle rather than cell growth control.

Acknowledgments

We thank the *Caenorhabditis* Stock Center, which is funded by the National Center for Research Resources, for providing several of the stocks used in this work. We also thank Bruce Edgar, Cynthia Wagner, Mike Krause, Peter Jackson and members of the laboratory for helpful discussions and reading of the manuscript. This work was supported by NIH grant R01GM37706 to A.Z.F. and an NIH post-doctoral fellowship to J.L.Y.

References

Blumenthal, T., Steward, K., 1997. RNA processing and gene structure. In: Riddle, D.L., Blumenthal, T., Meyer, B.J., Priess, J.R. (Eds.), *C. elegans II*. Cold Spring Harbor Laboratory Press, Cold Spring Harbor.

Boxem, M., van den Heuvel, S., 2001. lin-35 Rb and cki-1 Cip/Kip cooperate in developmental regulation of G1 progression in *C. elegans*. Development 128, 4349–4359.

Brenner, S., 1973. The genetics of *Caenorhabditis elegans*. Genetics 77, 71–94.

Chan, A.P., Etkin, L.D., 2001. Patterning and lineage specification in the amphibian embryo. Curr. Top. Dev. Biol. 51, 1–67.

Chitwood, B.G., Chitwood, M.B., 1950. An introduction to nematology. Monumental Printing Co, Baltimore.

Fares, H., Greenwald, I., 2001a. Genetic analysis of endocytosis in *Caenorhabditis elegans*: coelomocyte uptake defective mutants. Genetics 159, 133–145.

Fares, H., Greenwald, I., 2001b. Regulation of endocytosis by CUP-5, the *Caenorhabditis elegans* mucolipin-1 homolog. Nat. Genet. 28, 64–68.

Fay, D.S., Han, M., 2000. Mutations in *cye-1*, a *Caenorhabditis elegans* cyclin E homolog, reveal coordination between cell-cycle control and vulval development. Development 127, 4049–4060.

Greenwald, I., Seydoux, G., 1990. Analysis of gain-of-function mutations in the *lin-12* gene of *Caenohabditis elegans*. Nature 346, 197–199.

Harfe, B.D., V.G.A., Kenyon, C., Liu, J., Krause, M., Fire, A., 1998. Analysis of a *Caenorhabditis elegans* twist homolog identifies conserved and divergent aspects of mesodermal patterning. Genes Dev. 12, 2623–2635.

Hedgecock, E.M., White, J.G., 1985. Polyploid tissues in the nematode *C. elegans*. Dev. Biol. 107, 128–133.

Herman, R.K., Horvitz, H.R., Riddle, D.L., 1980. Genetic maps 1. The Nematode *Caenorhabditis elegans.* pp. 183–193.

Hodgkin, J., Horvitz, H.R., Brenner, S., 1979. Nondisjunction mutants of the nematode *Caenorhabditis elegans*. Genetics 91, 67–94.

Kostas, S.A., Fire, A., 2002. The T-box factor MLS-1 acts as a molecular switch during the specification of nonstriated muscle in *C. elegans*. Genes Dev. 16, 257–269.

Lazaro, J.B., Bailey, P.J., Lassar, A.B., 2002. Cyclin D-cdk4 activity modulates the subnuclear localization and interaction of MEF2 with SRC-family coactivators during skeletal muscle differentiation. Genes Dev. 16, 1792–1805.

Roca, X., Sachidanandam, R., Krainer, A.R., 2003. Intrinsic differences between authentic and cryptic 5′ splice sites. Nucleic Acids Res. 31, 6321–6333.

Park, M., Krause, M.W., 1999. Regulation of postembryonic G(1) cell cycle progression in *Caenorhabditis elegans* by a cyclin D/CDK-like complex. Development 126, 4849–4860.

Sulston, J.E., Horvitz, H.R., 1977. Post-embryonic cell lineages of the nematode *Caenorhabditis elegans*. Dev. Biol. 56, 110–156.

Sulston, J.E., Schierenberg, E., White, J.G., Thomson, J.N., 1983. The embryonic cell lineage of the nematode *Caenorhabditis elegans*. Dev. Biol. 100, 64–119.

Thorpe, C.J., Schlesinger, A., Carter, J.C., Bowerman, B., 1997. Wnt signaling polarizes an early *C. elegans* blastomere to distinguish endoderm from mesoderm. Cell 90, 695–705.

Zhang, J.M., Zhao, X., Wei, Q., Paterson, B.M., 1999. Direct inhibition of G(1) cdk kinase activity by MyoD promotes myoblast cell cycle withdrawal and terminal differentiation. EMBO J. 18, 6983–6993.